Effect of Metallic Ion Implantation on Dark Current Distributions of Silicon-Based CMOS Image Sensors

Juan Esteban Montoya Cardona, Sylvain Joblot, Pierre Kermagoret, Grégoire Ducotey, Stéphane Hardillier, Guillaume Dupeux, Yannick Borde, Jean-Pierre Carrère, Sandrine Lhostis, Richard Monflier, et al.

▶ **To cite this version:**

Juan Esteban Montoya Cardona, Sylvain Joblot, Pierre Kermagoret, Grégoire Ducotey, Stéphane Hardillier, et al.. Effect of Metallic Ion Implantation on Dark Current Distributions of Silicon-Based CMOS Image Sensors. 2024 IEEE SENSORS, Oct 2024, Kobe, Japan. 10.1109/SENSORS60989.2024.10784529 . hal-04888080

HAL Id: hal-04888080
https://laas.hal.science/hal-04888080v1

Submitted on 23 Jan 2025

HAL is a multi-disciplinary open access archive for the deposit and dissemination of scientific research documents, whether they are published or not. The documents may come from teaching and research institutions in France or abroad, or from public or private research centers.

L'archive ouverte pluridisciplinaire **HAL**, est destinée au dépôt et à la diffusion de documents scientifiques de niveau recherche, publiés ou non, émanant des établissements d'enseignement et de recherche français ou étrangers, des laboratoires publics ou privés.

Effect of metallic ion implantation on dark current distributions of silicon-based CMOS image sensors

Juan Esteban Montoya Cardona[1,2,3,*], Sylvain Joblot[1], Pierre Kermagoret[1], Grégoire Ducotey[1], Stéphane Hardillier[1], Guillaume Dupeux[1], Yannick Borde[1], Jean-Pierre Carrère[1], Sandrine Lhostis[1], Richard Monflier[2], Olivier Marcelot[3], Vincent Goiffon[3]

[1]STMicroelectronics, Crolles, France [2]LAAS-CNRS, Toulouse, France

[3]ISAE-SUPAERO, Université de Toulouse, Toulouse, France

[*]E-mail address of the corresponding author: Juan.MONTOYA-CARDONA@isae-supaero.fr

***Abstract*—Accidental metallic contamination is known to have a deleterious impact on the dark current characteristics of silicon-based CMOS image sensors (CIS), especially when metallic species are present in the depletion region of the photodiode. Solving a contamination issue requires a clear identification of the contaminant signature on the sensor response. In this study, different metallic species were voluntarily introduced in the photodiode region of Si-based CIS wafers, using ion implantation at relatively low doses. The dark current spectroscopy (DCS) technique is used to quantify the influence of each of these metallic species on the sensor performance. The results presented herein could aid in their identification after accidental contamination in a clean room environment, particularly in the cases of Pd, Mn and Nb, for which the references in the literature are scarce.**

Keywords—CMOS image sensors; dark current; metallic contamination.

I. INTRODUCTION

The accurate detection of photons in silicon-based CMOS image sensors (CIS) for a wide range of applications necessitates the use of high purity silicon (Si), i.e., with the smallest concentrations of impurities as possible. Metallic contaminants are particularly troublesome due to the introduction of deep electronic levels close to the middle of the Si bandgap [1], allowing them in many cases to act as significant Shockley-Read-Hall (SRH) generation-recombination centers and perturbing the normal operation of CIS devices due to the generation of current under no illumination, i.e. dark current, especially at high temperatures [2]. The impact of accidental metallic contamination on both CIS and other Si-based devices has long been known in the semiconductor industry, and significant efforts have been made to minimize the presence of undesired metallic species in the resulting devices and fabrication equipments [3].

Despite these efforts, different metals must still be used during a plethora of processing bricks, such as metallic interconnections, silicides and others [4]. The isolation between these structures and the bulk depletion region of the photodiode is therefore of paramount importance. Trace amounts of metallic contaminants can nevertheless be accidentally introduced in the critical region of the pixel, particularly in the case of ion implantation steps, as has been shown to be the case of W and Mo ions, for which the mass filtering can in some cases be quite tricky [5-6]. Even small concentrations of metallic contaminants in the pixels can render the CIS no longer suitable for their respective applications [7].

In this study, we present the dark current spectroscopy (DCS) results of Si-based CIS wafers voluntarily contaminated with different metallic species using ion implantation at relatively low doses and with energies necessary for an as-implanted peak concentration close to the photodiode junction line. Among the four metals detailed in this paper, only the impact of Au on the DCS spectra of Si-based CIS has already been studied experimentally in the literature [8]. This is not the case for Pd, Mn and Nb, for which we show a non-negligible impact on the DCS spectra, especially in the case of Nb. These results can be used for the identification of metals accidentally introduced into the Si substrate during the device fabrication.

II. EXPERIMENTAL PROCEDURE

Eleven metallic species were selected to be implanted at the photodiode level of CIS fabricated on 300 mm-diameter Si wafers. For each of the selected species, the implantation energy was determined with the aid of TCAD (Technology Computer-Aided Design) simulations with a projected range close to the PN junction of the photodiode. Moreover, two different implantation doses were used, henceforth called dose A and dose B, equivalent to 10 times dose A. The choice of the dose for each species was mainly motivated by their diffusivities in Si, as reported in [1,6,9-11], with most of the fast diffusers being implanted with the higher dose. A summary of the species as well as their implantation conditions is shown in Table I.

The wafers were prepared following a standard CIS process up to the photolithography level of the P^+ pinning ion implantation of the photodiode. After this P^+ pinning implantation, the metallic ion implantations were carried out using the same photoresist. The metal-implanted region corresponded to a 200 mm diameter circle centered on the 300 mm wafers, leaving a non-implanted reference 50 mm-wide annular region at the edge of the wafers. An appropriate wet cleaning of the frontside of the wafers was performed to reduce the accidentally induced surface metal contamination. Afterwards, the wafers were processed with the remaining steps of the fabrication route, including different thermal budgets.

TABLE I. METALLIC ION IMPLANTATION CONDITIONS

Metallic species	Implantation energy (keV)	Implantation dose (cm^{-2})	Diffusivity in Si at 1100 °C (cm^2/s)
Fe	110	B	4.15E-06 [1]
Cr	110	B	2.33E-06 [1]
Ti	100	A	3.91E-09 [1]
Mn	110	B	3.36E-06 [1]
Pd	190	A	4.43E-05 [1]
W	25	A	7.58E-14 [1]
	190		
Mo	180	A	2.19E-09 [6]
Au	190	A	8.89E-06 [1]
Zn	130	B	1.05E-07 [1]
Sn	190	B	~1-3E-15 [10,11]
Nb	180	A	~1E-07 [9]

Dark images of all the CIS dies in the wafers were acquired at 60 °C using integration times of 300 ms and 10 ms. The dark current of each pixel was estimated based on the subtraction of the two images. For each wafer, dark current distributions are extracted by averaging all dies in the implanted zone (COW for center of wafer) and the non-implanted reference zone (EOW for edge of wafer), excluding an intermediary 1 cm-wide buffer zone between these two; the populations are normalized by the number of dies in each zone. Afterwards, a ratio of the normalized pixel populations in the COW implanted region and the EOW reference region is calculated for each wafer (y-axis in figures 2-5).

III. RESULTS

The mean pixel populations with dark current above 200 a.u. for each wafer are shown in Fig. 1. This allows for a first overview of the impact of the implanted contaminants (grouped by dose) on the number of pixels with intermediate and high dark current values. In the cases of Fe, Cr and Ti, this impact is negligible, which is also confirmed when observing their practically identical dark current distributions, not shown here. For Mn, Pd and Sn, there is a non-negligible impact that remains quite moderate. In contrast, the remaining species (Zn, Au, Nb, W and Mo) show a significant 1 decade or more increase in the number of these pixels, with stark differences in the dark current histograms. This study will detail the results for Pd, Mn, Au and Nb implantations.

In the case of palladium implantation, as illustrated in Fig. 2, the increase for low dark current values representing the main intrinsic population remains negligible, with the exception of the region between ~50 a.u. and ~100 a.u., for which the population doubles. For this species, the main observed impact pertains to the hot pixel exponential tail at dark current levels above ~450 a.u., in which an enhancement with a factor between 3 and 4 is observed. While scarcely studied in the literature, the moderate impact evidenced in Fig. 2 may be explained by the nature of Pd atoms as a fast diffuser (at least 10 times faster than Fe atoms) [1].

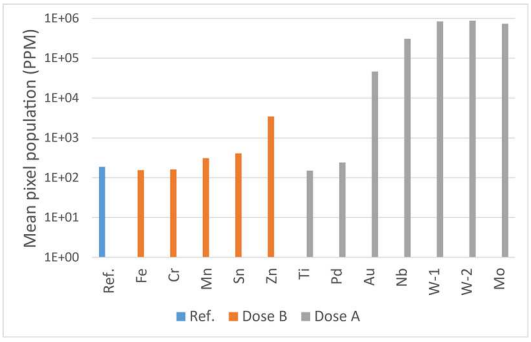

Fig. 1. Mean pixel population with dark current above 200 a.u.. W-1 and W-2 refer to tungsten implanted at energies of 25 keV and 190 keV, respectively. Ref. corresponds to the EOW region of the Fe-implanted wafer.

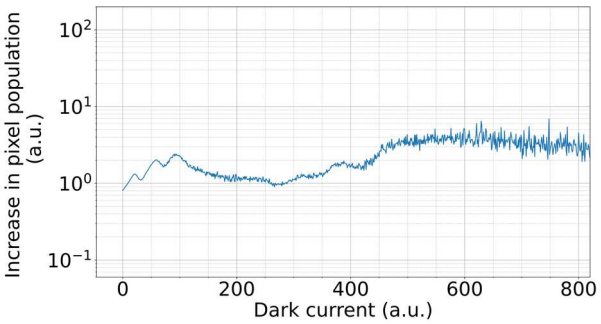

Fig. 2. Relative dark current distribution for wafer implanted with Pd.

In contrast to the case of Pd, some other species introduced well defined peaks that may act as a signature in DCS data, allowing for their identification. The first of these species is manganese, for which the relative distribution is shown in Fig. 3., with a new peak at ~223 a.u. No other prominent impact is observed in the dark current distribution, including the hot pixel tail which remains unmodified. Overall, the impact of manganese ions on dark current, only estimated in the literature theoretically but not experimentally [12], is quite moderate, as expected for a fast diffuser.

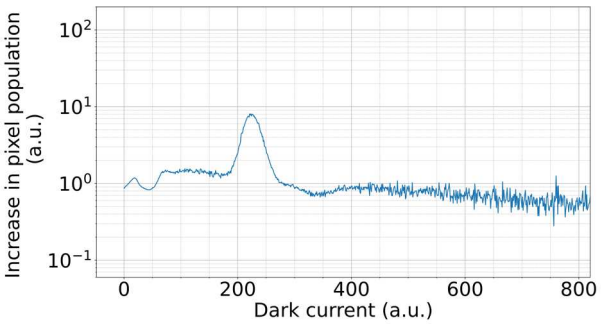

Fig. 3. Relative dark current distribution for wafer implanted with Mn.

The second species for which defined peaks appear is gold, as illustrated in Fig. 4, with two peaks positioned at dark current levels of ~284 a.u. and ~558 a.u., as well as a third peak at ~833 a.u., partially obstructed by the saturation observed at the end of the distribution. These 3 peaks are equidistant and decreasing in amplitude. On top of this, a significant tenfold or more increase is perceived

for pixels with low and intermediate dark current values, whereas the hot pixel tail above ~450 a.u. presents a more moderate increase. Despite the high diffusivity of Au in Si, it has already been shown [8] to have a deleterious impact in the dark current characteristics of CIS, possibly due to a preferential interaction between Au atoms and Si vacancies, coupled with at least one deep acceptor level [1,8].

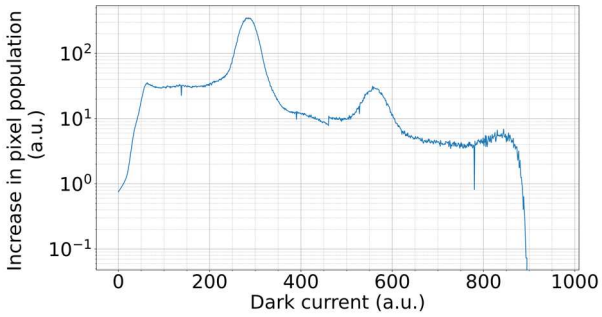

Fig. 4. Relative dark current distribution for wafer implanted with Au.

The third and final species which shows clear peaks is niobium, as shown in Fig. 5, with two peaks situated at ~390 a.u. and ~752 a.u., respectively. Despite the saturation gauged at the end of the distribution, the impact of Nb contamination on the dark current spectrum is dramatic, with a strong two decades or more increase in the population of pixels with dark current above ~60 a.u. No other studies have been found in the literature on the impact of Nb contamination on the dark current of Si-based CIS. It has however been shown to cause a significant degradation in the performance of solar cells [13]. This can in part be explained by its classification as an intermediate diffuser, as well as by the introduction of at least one deep donor level for interstitial Nb [1].

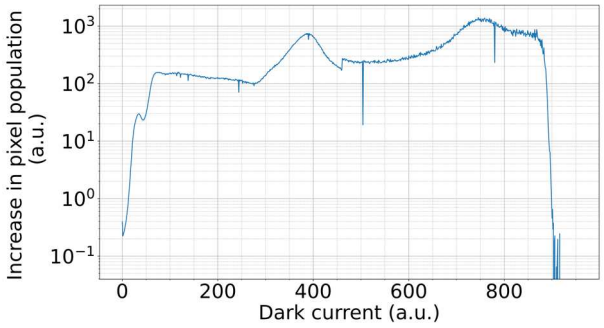

Fig. 5. Relative dark current distribution for wafer implanted with Nb.

Among the remaining seven metals included in Table I but not detailed in this paper, all of them with the exception of Fe, Cr and Ti were shown to have non-negligible degrees of impact on the DCS characteristics of the CIS wafers, in qualitative agreement with the available literature [2,8,14].

IV. Discussion

It can be ascertained from the literature that two of the main factors that determine the impact of a metallic contaminant on the dark current characteristics of Si-based CIS are their diffusivities in Si, as well as the introduction of discrete energy levels close to the Si midgap, allowing them to act as efficient SRH centers. In regard to the diffusivity aspect, among the four metallic species described in this paper, the slowest diffuser (niobium) is indeed the one with the most notorious impact on the CIS dark current distribution. The results for manganese and especially gold might seem unintuitive, as they were shown to have a considerable impact on the DCS spectra despite their classification as fast diffusers. This can however be explained by the aforementioned second factor, being the presence of levels close to the Si midgap for both species [1,8,12]. Even a small number of metallic contaminants not having diffused out of the photodiode depletion region could therefore be enough to contribute to a significant dark generation current.

Despite not being as prevalent as other contaminants such as Mo or W in ion implanters [2,15-16], some overlooked contaminants can still potentially be present in trace amounts in a clean room environment. For instance, Pd, Mn and Nb could respectively be found during the fabrication of interconnectors, ferroelectric memories or low resistivity metallic gates [17]. In spite of the prevalence of good practices, risks of cross-contamination cannot always be excluded, and the dark current characteristics presented in this study could be of great interest for helping in the identification of metallic impurities accidentally introduced during the fabrication of CIS. This is especially true in the case of contaminants that we have shown to present clear peaks in the relative DCS spectra, as is the case for Mn, Au, and Nb. In the case of Au, the observed quantization of equidistant peaks suggests a subjacent Poisson distribution of metallic atoms in the pixel matrix [8]; the three peaks observed in Fig. 4 could therefore be attributed to pixels containing 1, 2 and 3 Au atoms in their active volume, respectively.

V. Conclusion

Dark current measurements were performed at 60 °C on Si-based CIS wafers implanted close to photodiode junction using different metallic species, at relatively low doses. All of the four metals presented in this paper (Pd, Mn, Au and Nb) were shown to have varying impacts on the dark current characteristics of the device, with the most deleterious one being that of Nb contamination, possibly ascribed to its relatively low diffusivity, allowing it to remain in non-negligible concentrations in the depletion region after different post-implantation anneals. In the cases of Mn, Au and Nb contamination, the observation of defined peaks provides a means for their identification during accidental contamination; for Au contamination, the peaks seem to be equidistant and quantized, showing evidence of a Poisson distribution of Au atoms in the pixel matrix. In our knowledge, the impact of Pd, Mn and Nb on the DCS characteristics of Si-based CIS has not been previously studied experimentally in the literature.

REFERENCES

[1] K. Graff, *Metal Impurities in Silicon-Device Fabrication*, 2nd ed. in Materials Science. Springer, 2000.

[2] M. L. Polignano, F. Russo, G. Moccia, and G. Nardone, "Analysis of the dark current distribution of CMOS image sensors in the presence of metal contaminants," *Semicond. Sci. Technol.*, vol. 35, no. 124003, pp. 1–10, 2020, doi: https://doi.org/10.1088/1361-6641/abb840.

[3] J.-P. Carrère, S. Place, J.-P. Oddou, D. Benoit, and F. Roy, "CMOS Image Sensor: Process impact on Dark current," presented at the IEEE International Reliabilty Physics Symposium, Waikoloa, HI: IEEE, 2014, pp. 1–6.

[4] M. Grégoire, "Silicides in microelectronics: phase sequence, nanoscale effect and degradation mechanisms," Postdoctoral Thesis, Aix-Marseille Université, 2021.

[5] R. B. Liebert, G. C. Angel, and M. Kase, "Tungsten Contamination in BF2 Implants," presented at the 11th International Conference on Ion Implantation Technology, 1996, pp. 135–138.

[6] J. L. Benton *et al.*, "Behavior of Molybdenum in Silicon Evaluated for Integrated Circuit Processing," *Journal of The Electrochemical Society*, vol. 146, no. 5, pp. 1929–1933, 1999.

[7] F. Domengie, P. Morin, and D. Bauza, "Modeling the dark current histogram induced by gold contamination in complementary-metal-oxide-semiconductor image sensors," *J. Appl. Phys.*, vol. 118, no. 024501, pp. 1–10, 2015, doi: http://dx.doi.org/10.1063/1.4922969.

[8] F. Domengie, J. L. Regolini, and D. Bauza, "Study of Metal Contamination in CMOS Image Sensors by Dark-Current and Deep-Level Transient Spectroscopies," *Journal of ELECTRONIC MATERIALS*, vol. 39, no. 6, pp. 625–629, 2010.

[9] M. L. Polignano *et al.*, "Niobium Contamination in Silicon," *ECS Transactions*, vol. 33, no. 11, pp. 133–144, 2010, doi: 10.1149/1.3485688.

[10] T. H. Yeh, S. M. Hu, and R. H. Kastl, "Diffusion of Tin into Silicon," *Journal of Applied Physics*, vol. 39, no. 9, pp. 4266–4271, 1968.

[11] P. Kringhøj and A. N. Larsen, "Anomalous diffusion of tin in silicon," *PHYSICAL REVIEW B*, vol. 56, no. 11, pp. 6396–6399, 1997.

[12] P. W. Mertens, S. Lavizzari, and S. Guerrieri, "Specification of Trace Metal Contamination for Image Sensors," *Solid State Phenomena*, vol. 255, pp. 309–312, 2016, doi: 10.4028/www.scientific.net/SSP.255.309.

[13] Hopkins, R. H., Davis, J. R., Rohatgi, A., Hanes, M. H., Rai-Choudhury, P., and Mollenkopf, H. C., "SILICON MATERIALS TASK OF THE LOW COST SOLAR ARRAY PROJECT - Effect of Impurities and Processing on Silicon Solar Cells," US Department of Energy, 1982.

[14] F. Russo *et al.*, "Dark Current Spectroscopy of Transition Metals in CMOS Image Sensors," *ECS Journal of Solid State Science and Technology*, vol. 6, no. 5, pp. 217–226, 2017, doi: 10.1149/2.0101705jss.

[15] F. Domengie, J. L. Regolini, D. Bauza, and P. Morin, "Impact on Device Performance and Monitoring of a Low Dose of Tungsten Contamination by Dark Current Spectroscopy," *IEEE International Reliability Physics Symposium*, p. 6, 2010.

[16] E. A. G. Webster, R. L. Nicol, L. Grant, and D. Renshaw, "Per-Pixel Dark Current Spectroscopy Measurement and Analysis in CMOS Image Sensors," *IEEE TRANSACTIONS ON ELECTRON DEVICES*, vol. 57, no. 9, 2010, doi: 10.1109/TED.2010.2052399.

[17] F. Domengie, "Etude des défauts électriquement actifs dans les matériaux des capteurs d'image CMOS," PhD Thesis, Université de Grenoble, 2011.